5-2010

Bistability in Differential Equation Model of Oyster Population and Sediment Volume

William Crowell Jordan-Cooley
College of William and Mary

Bistability in Differential Equation Model of Oyster Population and Sediment Volume

A thesis submitted in partial fulfillment of the requirement
for the degree of Bachelors of Science in Mathematics from
The College of William and Mary

by

William Crowell Jordan-Cooley

Accepted for _____

_____
Junping Shi, Director

_____
Rex Kincaid

_____
Romuald Lipcius

_____
Leah Shaw

_____
Jian Shen

Williamsburg, VA
April 21, 2010

Bistability in Differential Equation Model of Oyster Population and Sediment Volume

William Crowell Jordan-Cooley

Email: wcjord@wm.edu

April 21, 2010

Abstract

The Chesapeake Bay oyster has been the focus of more than a century of heavy harvesting and now several decades of restoration attempts. Concerted efforts to rebuild the native oyster population and reef structure have yielded limited results. Recent success in the Great Wicomico River suggests that initial reef height combats growth retarding sedimentation resulting in multiple stable states of reefs. We use a system of three differential equations to model volumes of live oysters, dead oysters, and sediment. We show that multiple nonnegative equilibria exist for an ecologically reasonable range of parameters and the initial height of oyster reefs determines which equilibria is reached.

Contents

List of Figures

Chapter 1

Introduction

1.1 Background

It is 1650 and you stand on the deck of a sailing vessel traveling up the James River towards Jamestown. You peer into the depths and see the glory of the Chesapeake Bay ecosystem as we can only imagine it today. At the bottom are the dominant engineers of this ecosystem, *Crassostrea virginica*, the native Chesapeake Bay oyster. Bivalve mollusks, they live on reefs created over time which are so large that they pose navigation hazards to passing ships (Newell, 1988). The enormous reef structure suppresses sediment resuspension, provides habitat for other species, and elevates the oysters into the areas of highest water flow. They are quietly filtering the water and extracting their prize, phytoplankton. They deal with sediment and nutrients in turn, wrapping them in mucus and discarding them as pseudofeces (Lenihan et al., 1999). Swiftly and surely, they will filter the bay, controlling the levels of phytoplankton and sediment (Newell, 1988).

This scene is all but gone today. The past century has seen an industry of oysters rise and fall and with it have gone approximately 99 percent of the Bay's oysters (Schulte et al., 2009). Harvests peaked in 1884 at 615,000 metric tons, shortly after the introduction of power dredges. By 1992, the harvest was 12000 metric tons (Rothschild et al., 1994).

Figure 1.1: (left) high relief reef (HRR); (middle) low relief reef (LRR); (right) unrestored bottom (UNB). From (Schulte, et.al. 2009).

Additionally, human activities on land have increased the flow of sediment into the bay's waters (Newell, 1988). The increase in sediment has weakened the oysters, lowering fecundity and raising mortality (Rothschild et al., 1994; Schulte et al., 2009; Lenihan et al., 1999). Exacerbating the situation, the physical profile of reefs has been leveled, placing the oysters lower in the water column where water flow is reduced and sediment chokes all but a few fortunate individuals (Newell, 1988; Lenihan, 1999; Shulte et al., 2009).

Efforts to restore native oyster populations have been extensive but largely ineffectual (Ocean Studies Board, 2004). However, a recent restoration effort in the Great Wicomico River has yielded promising results. In 2004, the Army Corps of Engineers created more than 80 acres of reef in the Great Wicomico River consisting of oyster shell planted at different reef heights. The field experiment featured high-relief reefs (HRR) built at an average of $25 - 42$ cm in height, low-relief reefs (LRR) at $8 - 12$ cm, and a control of unrestored bottom (UNB). After three years, in 2007, the higher reefs (HRR) were considerably more successful. Mean oyster density was fourfold higher on HRR (1026 ± 51.5 SE) than LRR (250.4 ± 32.3 SE). In contrast, the average density in Chesapeake Bay sanctuary reefs was $100 - 152$ oysters per squared meter (Schulte et al., 2009), see Figure 1.1.

The dramatic decline in the oyster population as well as the marked difference in suc-

cess of the high relief and low relief reefs may be explained in the context of catastrophic shifts and bistability. Some systems exhibit precipitous shifts in state without correspondingly dramatic changes in external conditions (Scheffer et al, 2001). Such shifts have been observed in oceans, lakes, coral reefs, and the Sahara Desert. Gradual changes in the external conditions of a system produce correspondingly gradual changes in state variables until sudden drastic changes occur. After the degraded state has been reached, a return to the external conditions present before the change does not return the system to the pre-shift state. These systems have a property called bistability (Scheffer et al., 2001; Guill, 2009). Bistability (i.e. alternative stable states) is the existence of multiple equilibria within a system. These equilibria exist for a non-vanishing range of constant external environmental conditions (Guill, 2009).

1.2 Bistability

Alternative stable states are generally due to one or more feedback mechanisms (Scheffer et al., 2001; Guill, 2009). In the Chesapeake Bay, oysters filter the sediment flowing onto reefs, which may prevent high turbidity levels. Historically, massive reductions in oyster biomass and degradation of the reef matrix contributed to increasing sediment in the water column (Newell, 1988). Additionally, oysters encounter a greater proportion of the sediment in the water column when they are closer to the bottom, which occurs with reductions in the vertical relief of reefs. The sediment negatively affects oysters by causing them to expend energy to filter it, thereby increasing susceptibility to disease and mortality rates while decreasing growth and reproduction. Raising the oysters in the water column can lead to higher fecundity and decreased mortality from reductions in turbidity and elevated filtration rates (Rothschild et al., 1994; Lenihan et al., 1999; Ocean Studies Board, 2004).

The ecosystem properties of shallow lakes are similar to those of Chesapeake Bay. In shallow lakes, aquatic vegetation dampens resuspension of sediment, reduces nutrients in

the water column, and provides protection from fish predation for zooplankton that feed on phytoplankton. Fish control zooplankton and resuspend sediment and nutrients by disturbing the lake floor (Scheffer, 2009).

However, aquatic vegetation and zooplankton have been depleted by herbicides and pesticides. The reduction in vegetation leads to an increase in nutrients in the water column which increases phytoplankton, which in turn feed on the nutrients. Declines of zooplankton result in unchecked growth of phytoplankton. A dramatic increase in phytoplankton precludes light from reaching the lake floor which causes the vegetation to decline further. This exposes zooplankton to increased predation, which in turn leads to lower predation pressure on phytoplankton (Scheffer, 2009).

It has been possible to return the lakes to a state of high vegetation and controlled phytoplankton abundance. However, the zooplankton population must be rebuilt to a critical level such that they can control phytoplankton, allow aquatic vegetation to return, and thus facilitate the profusion of vegetation that provides protection from fish predation. To do so, herbicides and pesticides must be stemmed. Then by temporarily reducing the number of fish, zooplankton proliferate due to the abundance of phytoplankton as prey. Once phytoplankton are reduced, the vegetation can become re-established. Increases in zooplankton eventually allows the fish population to rebound, restoring the system to the pristine stable state (Scheffer, 2009).

The oyster reef system is analogous to that of shallow lakes. Oysters can control the volume of sediment and phytoplankton, but they must first be provided with optimal reef features. The experimental results from the Great Wicomico River provide evidence of hysteresis. We now provide the theoretical underpinnings that the interaction of oysters and sediment can produce alternative stable states of oyster reef populations in Chesapeake Bay.

1.3 Bifurcation Theory

Bifurcation theory is the mathematical study of qualitative or structural changes in the dynamical behavior of natural or engineered systems. A bifurcation occurs when some certain physical parameters cross through critical thresholds. The word "bifurcation" is from the Latin *bifurcus*, which means 'two forks', and one of the fundamental bifurcation types is the pitchfork bifurcation (Chow and Hale, 1982; Wiggins, 1991).

A typical bifurcation occurs when the stability of a known trivial equilibrium solution changes as a parameter changes, and non-trivial equilibrium solutions emerge from the branch of the trivial equilibrium solutions. If the new non-trivial equilibrium solution is stable, then the local stable state of the system switches from the trivial one to the non-trivial one. But if the bifurcating equilibrium point is unstable, the trivial state remains stable for that parameter range, then often there exists another non-trivial stable state. Hence a pair of alternative stable states is the result of such a bifurcation of unstable equilibrium states, which is often called a "backward bifurcation" in literature, especially the studies of epidemics (Hadeler and Van den Driessche, 1997).

To determine the bifurcation direction of the branch of non-trivial solutions, one can use a classical bifurcation theorem (Crandall and Rabinowitz, 1971; Shi 1999; Liu et.al. 2007), which will be recalled in Section 3.3. Note that in earlier work, a cusp type bifurcation occurs when a system parameter changes to produce a S-shaped bifurcation diagram, and a hysteresis loop is generated as a result. That has been used to explain many catastrophic shifts in the natural world (Scheffer et al., 2001; Scheffer, 2009). A mathematical survey on catastrophic shifts and bistability can be found in (Jiang and Shi, 2009). The bifurcation diagram in this paper is not S-shaped and the lower stable state is the trivial one, but the bistability mechanism is similar.

Usually the bistable structure is sensitive to the initial values of the system. A small perturbation of the initial value could change the eventual outcome from one stable state to a different one, which is called "hair-trigger effect". In general the basins of attraction

of the two stable states are only separated by a surface in the phase space (Jiang and Shi, 2009). This is also evident from numerical simulations of the oyster population model here.

1.4 Summary of results

We will construct a model of differential equations to demonstrate that the mechanisms involved in the interaction of oysters and sediment produce bistability and explain the success of high relief reefs in the context of multiple stable states. Analysis will show that sediment deposition rates and the initial height of artificial reefs play a dominant role in the long term behavior of reefs.

Chapter 2

Mathematical Model

We model the change of live oyster, dead oyster, and deposited sediment volume with respect to time, t, measured in years. The live oysters will grow according to logistic growth but be negatively affected by sediment volume. We will introduce a function, $f(d)$, to represent the proportion of oysters above the level of fatal sediment. The change in dead oyster volume will be the deaths of live oysters minus a degradation rate proportional to dead oyster volume. The volume of sediment deposited on the reef will be a constant maximum sediment scaled a function, $g(O + B)$, depending on the position of the reef in the water column and a function, $F(x)$, yielding the filtration by live oysters.

The differential equation model has three variables as in the following table:

Variable Name	*Variable meaning*	*Dimension*	*Variable defining domain*
t	time	years	$t \geq 0$
$O(t)$	live oysters	m^3	$O \geq 0$
$B(t)$	dead oysters	m^3	$B \geq 0$
$S(t)$	sediment	m^3	$S \geq 0$

Table 2.1: Table of variables in the equations.

We first explain the function $f(d)$ which represents the proportion of oysters not affected by sediment. The input, d, represents the volume of the live (O) and dead (B) oysters not affected by sediment (S). Hence we define

$$d = \lambda\,(O + B) - S. \tag{2.1}$$

The packing density $0 \leq \lambda \leq 1$ indicates that the stacking oyster shells may not occupy all space. Note that the volume is essentially height multiplied by a unit surface area, so d can be understood as the height of the oysters above the sediment.

We assume that $f(d)$ is a positive, increasing and continuously differentiable function defined on $(-\infty, \infty)$ with a sigmoid shape bounded by 0 and 1. $d = \lambda O$ when the dead oysters are covered by sediment but the live oysters are not; $\lambda B = S$. In this situation, minimal oysters are affected by sediment and $f(\lambda O) \approx 1$. $d = 0$ when both live and dead oysters are inundated by sediment. Hence, $f(0) \approx 0$. As d approaches the positive and negative limits, the approximations are equalities. Summarily,

$$f'(d) > 0, \quad f(0) \approx 0, \quad f(\lambda O) \approx 1, \quad \lim_{d \to -\infty} f(d) = 0, \quad \text{and } \lim_{d \to \infty} f(d) = 1. \tag{2.2}$$

The change in live oyster volume $O(t)$ is represented by a differential equation:

$$\frac{dO}{dt} = rOf(d)\left(1 - \frac{O}{k}\right) - \mu f(d)O - \epsilon(1 - f(d))O. \tag{2.3}$$

Here the live oyster is assumed to have a logistic growth. r represents the intrinsic birth rate per cubic meter of oyster volume. The oyster population increases at a decreasing density dependent rate until the population reaches the carrying capacity k. In the second term of the equation, μ is the natural death rate of the oyster. Both terms are scaled by $f(d)$ because oysters covered in sediment will not reproduce or die by natural causes. The third term represents the decrease in live oyster volume as a result of sediment, and ϵ is the death rate of submerged oysters. As $f(d)$ goes to 1, the term goes to zero. However, as $f(d)$ becomes smaller, the term begins to have more significance.

The second differential equation which shows the change of dead oyster volume $B(t)$ is

$$\frac{dB}{dt} = \mu f(d)O + \epsilon(1 - f(d))O - \gamma B. \tag{2.4}$$

The first two terms are directly from dying live oyster in equation (2.3), and the third term is the loss of dead oyster volume due to the degradation of shell. This loss is proportional to the volume of dead oysters at the rate of γ. Note that another loss term $rO^2 f(d)/k$ in (2.3) is not included in (2.4) as it is the loss due to interspecific competition, and it does not increase the dead oyster volume as the other two terms.

Finally the system of differential equations is completed by a third equation describing the change of sediment volume $S(t)$:

$$\frac{dS}{dt} = -\beta S + Cge^{-\frac{FO}{Cg}}. \tag{2.5}$$

Here the first term is the volume of sediment eroded which is proportional to the volume of deposited sediment at a rate β; the second term is the rate of the sediment volume being deposited. The sediment deposition rate in the absence of oysters is Cg, where C is a maximum deposition rate and g is a modification that depends on reef height $O + B$. The deposition rate is at maximum when the reef is in nonexistence and it decreases as the reef height in the water column increases. Hence with the reef height represented by $x = O + B$, we assume that the function $g(x) = g(O + B)$ satisfies

$$g(0) = 1, \;\; g'(x) \leq 0, \;\; x \geq 0, \quad \text{and} \quad \lim_{x\to\infty} g(x) = 0. \tag{2.6}$$

In the presence of (live and/or dead) oysters, the deposition term should be reduced by a multiplicative factor due to filtration. The filtration rate per unit oyster volume depends on the height-dependent sediment concentration Cg. It should scale linearly with Cg when Cg is small, reach a peak M at some optimal sediment concentration, and beyond this threshold, it decreases as oysters gills become increasingly clogged. (i.e., like

a Ricker function of sediment concentration). Hence $F = F(y) = F(Cg)$ satisfies

$$\begin{aligned} &F(0) = 0, \quad \lim_{y\to\infty} F(y) = 0, \quad \text{and there exists } \ y_0 > 0 \ \text{ such that} \\ &F'(y) > 0, \ \ 0 < y < y_0; \ \ F'(y) < 0, \ \ y > y_0, \ \ \text{and } \ F(y_0) = F_0. \end{aligned} \tag{2.7}$$

Both $g(x)$ and $F(y)$ are positive and continuously differentiable functions on $[0, \infty)$.

The derivation of (2.5) begins with a mass balance of sediment deposition in a control volume at the bottom (Chapra, 1997; Ji, 2008):

$$\frac{d(VC_s)}{dt} = \Omega_s A C_b - V_e A C_s - V_b A C_s - V_f O, \tag{2.8}$$

where Ω_s is settling velocity (m/day), V_e is erosion velocity (m/day), V_b is burial velocity (m/day), C_s is sediment concentration at the bottom sediment (g/m^3), C_b is the sediment concentration above the bottom sediment layer (g/m^3), V is the control volume, (m^3), A is the surface area, (m^2), of the control volume, V_f is the filtration rate (g/day), and O is live oyster volume, (m^3).

We introduce mean erosion rate $v_e(1/day)$ and burial rate $v_b(1/day)$, which can be considered to be a re-scaling of the erosion and burial velocities V_e and V_b by the mean depth, and write as follows:

$$\frac{d(VC_s)}{dt} = \Omega_s A C_b - v_e V C_s - v_b V C_s - V_f O. \tag{2.9}$$

The bottom sediment can be expressed as sediment density ρ and the porosity ϕ as $C_s = \rho(1-\phi)$ (Chapra, 1997). We assume that the mean porosity, $\bar{\phi}$, is a constant and divide (2.9) by $\rho(1-\bar{\phi})$. Let $S = \dfrac{V(1-\phi)}{1-\bar{\phi}}$ as the sediment volume with porosity normalized by the mean porosity to quantify the volume of unconsolidated sediment deposition at the bottom, and let $\omega_s = \dfrac{\Omega_s A}{\rho(1-\bar{\phi})}$ and $v_f = \dfrac{V_f}{\rho(1-\bar{\phi})}$. Then (2.9) can be written as

$$\frac{dS}{dt} = \omega_s C_b - v_e S - v_b S - v_f O. \tag{2.10}$$

Rearrangement of the terms in the equation makes it

$$\frac{dS}{dt} = \omega_s C_b (1 - \frac{v_f O}{\omega_s C_b}) - (v_e + v_b) S. \tag{2.11}$$

Here the first term shows the sediment deposition modified by oyster filtration, and the second term shows the combined loss of sediment due to erosion or burial. But the first term could be negative for large value of O, hence we replace the decreasing linear function $1 - \dfrac{v_f O}{\omega_S C_b}$ by a decreasing nonlinear function $\exp\left(\dfrac{-v_f O}{\omega_S C_b}\right)$ whose linearization is $1 - \dfrac{v_f O}{\omega_S C_b}$. Now we rename

$$\omega_S C_b = Cg, \quad \text{and} \quad v_f = F,$$

where C is a constant represents the maximum deposition rate, and g is a decreasing function of $O + B$ with maximum $g(0) = 1$, then we obtain (2.5). The estimates of C and g come from data of ω_S and C_b, information on v_f can be used to determine $F = Cge^{-\theta Cg}$, and finally v_e and v_b determine β.

We remark that the equation (2.5) has properties reflecting the qualifications of the system.

- When $O \to 0$, $\dot{S} \sim Cg - \beta S$ (deposition and erosion without oysters).

- When O is small, from a Taylor expansion of the exponential we have $\dot{S} \sim Cg - FO - \beta S$ so the deposition rate is being reduced linearly by whatever amount O oysters filter out.

- When $O \to \infty$, $\dot{S} \sim -\beta S$ (no deposition, only erosion). The negative is not a problem, since this stops decreasing at $S = 0$.

- When the filtration rate per unit oyster volume $F \to 0$, either because there is too little sediment to filter or the oysters are being choked by it, $\dot{S} \sim Cg - \beta S$.

In summary, we propose the following differential equation model for oyster population

and sediment growth:

$$\frac{dO}{dt} = rOf(d)\left(1 - \frac{O}{k}\right) - \mu f(d)O - \epsilon(1 - f(d))O, \tag{2.12}$$

$$\frac{dB}{dt} = \mu f(d)O + \epsilon(1 - f(d))O - \gamma B, \tag{2.13}$$

$$\frac{dS}{dt} = -\beta S + Cge^{-\frac{FO}{Cg}}, \tag{2.14}$$

where the quantities d, $f(d)$, $g = g(O + B)$ and $F = F(Cg)$ satisfy (2.2), (2.6) and (2.7) respectively. A set of functions satisfying these conditions will be given in Section 3.4. The parameters of the system (2.12)-(2.14) are summarized in Table 2.2.

Parameter	Meaning	Dimension	Value
r	birth minus death by competition rate	$(year)^{-1}$	$0.7 - 1.3$
k	oyster capacity	m^3	$0.1 - 0.3$
μ	natural death rate	$(year)^{-1}$	$0.2 - 0.6$
ϵ	death rate of submerged oyster	$(year)^{-1}$	0.94
λ	packing density	none	1
γ	oyster shell degradation rate	$(year)^{-1}$	$0.5 - 0.9$
F_0	maximum sediment filtration	$(year)^{-1}$	1
C	maximum sediment deposition rate	$m^3(year)^{-1}$	$0.04 - 0.08$
y_0	sediment amount where the filtration is maximum	$year \cdot m^{-3}$	0.02
β	sediment erosion rate	m^{-3}	$0.02 - 0.04$
h	scaling factor	m^{-3}	$10 - 30$
η	decay rate of sediment deposition on the reef height	m^{-3}	3.33

Table 2.2: Table of parameters in the equations.

The last two parameters h and η are specific to the choice of f and g, which will be explained in Section 3.4.

Chapter 3

Model Analysis

3.1 Solving for Equilibria

We are interested in determining the values of parameters and state variables at which the change in the state variables is equal to zero. In other words, what environmental conditions will result in an equilibrium reef-sediment system. To answer this question, we consider the equilibrium solutions of our model (2.12)-(2.14), which satisfy

$$0 = rOf(d)\left(1 - \frac{O}{k}\right) - \mu f(d)O - \epsilon(1 - f(d))O, \tag{3.1}$$

$$0 = \mu f(d)O + \epsilon(1 - f(d))O - \gamma B, \tag{3.2}$$

$$0 = -\beta S + Cge^{-\frac{FO}{Cg}}. \tag{3.3}$$

A trivial solution of (3.1) − (3.3) where $O = B = 0$ and $S = C/\beta$ is an equilibrium solution representing the extinction of the oyster population and the accumulation of sediment limited only by erosion. We will now solve the system in search of nontrivial solutions where $O > 0$, $B > 0$ and $S > 0$.

We describe a procedure of reducing the equations (3.1)-(3.3) to a single equation. From (3.1), we obtain (assuming $O > 0$)

$$f(d) = \frac{\epsilon k}{k(r - \mu + \epsilon) - rO}; \tag{3.4}$$

and similarly from (3.2), we obtain

$$f(d) = \frac{\gamma B - \epsilon O}{(\mu - \epsilon)O}. \tag{3.5}$$

From (3.4) and (3.5), we can have an equation of O and B only:

$$\frac{\epsilon k}{k(r - \mu + \epsilon) - rO} = \frac{\gamma B - \epsilon O}{(\mu - \epsilon)O}, \tag{3.6}$$

and B can be solve from (3.6) as

$$B = \frac{r\epsilon O(k - O)}{\gamma[k(r - \mu + \epsilon) - rO]} \equiv B(O). \tag{3.7}$$

On the other hand, one can solve S from (3.3):

$$S \equiv S(O, B) = \frac{C}{\beta} g e^{-FO/Cg}, \tag{3.8}$$

where g depends on $O + B$ and F depends on g. Now the substitution of (3.7) and (3.8) into (3.4) results in an implicit equation of O only:

$$f\left(\lambda\left(\frac{O}{2} + B(O)\right) - S(O, B(O))\right) = \frac{\epsilon k}{k(r - \mu + \epsilon) - rO}. \tag{3.9}$$

Hence for a fixed set of parameters, any root $O_* > 0$ of (3.9) corresponds to an equilibrium point $(O_*, B(O_*), S(O_*, B(O_*)))$ of (3.1)-(3.3). While direct analysis of (3.9) is not easy with complicated definitions of $O(B)$ and $S(O, B)$, numerical calculation of (3.9) is relatively easy with the help of a software such as `Maple` (see example given below).

We define the functions on the left and right hand side of (3.9) to be

$$L(O) = f\left(\lambda\left(\frac{O}{2} + B(O)\right) - S(O, B(O))\right), \tag{3.10}$$

$$R(O) = \frac{\epsilon k}{k(r - \mu + \epsilon) - rO}. \tag{3.11}$$

From (3.9), intersection points of the graphs of $L(O)$ and $R(O)$ are equilibrium points. We observe that $L(O)$ is bounded by 1 and $R(O)$ is unbounded as $O \to k_* = k(r - \mu + \epsilon)/r$, which is a modified carrying capacity. Thus if $L(0) > R(0)$, then (3.9) has at least one

root from intermediate-value theorem; and if $L(0) < R(0)$, then (3.9) may have no or two zeros. It is easy to see that

$$L(0) = f(-C/\beta), \quad \text{and} \quad R(0) = \frac{\epsilon}{r - \mu + \epsilon}.$$

3.2 Stability of Trivial Solution

From a different point of view, one can consider the equations (3.1)-(3.3) with bifurcation method and linearization. Linearizing (3.1)-(3.3) at the trivial equilibrium $(O, B, S) = (0, 0, C/\beta)$, we obtain the Jacobian matrix to be a diagonal one

$$J(0,0,C/\beta) = \begin{pmatrix} f(-C/\beta)(r-\mu+\epsilon) - \epsilon & 0 & 0 \\ f(-C/\beta)(\mu-\epsilon) + \epsilon & -\gamma & 0 \\ Cg'(0) - F(C) & Cg'(0) & -\beta \end{pmatrix}. \tag{3.12}$$

It is easy to observe that if $r < \mu$ (birth rate smaller than death rate), then the trivial one is the only equilibrium. In the following we assume that the parameters r, μ and ϵ satisfy

$$r > \mu, \text{ and } f(0)(r - \mu + \epsilon) > \epsilon. \tag{3.13}$$

Notice that the second condition in (3.13) suggests that ϵ is small. Also the condition (3.13) and the monotonicity of f assumed in (2.2) imply that there exists a unique $C_* > 0$ such that $f(-C/\beta)(r-\mu+\epsilon)-\epsilon > 0$ for $C > C_*$, and $f(-C/\beta)(r-\mu+\epsilon)-\epsilon < 0$ for $C < C_*$. Since the Jacobian matrix $J(0, 0, C/\beta)$ is lower triangular, then the three diagonal entries are eigenvalues. We have the following result regarding the stability of the trivial state and existence of equilibrium points:

Proposition 3.1. *Suppose that the conditions* (2.2), (2.6), (2.7) *and* (3.13) *are satisfied, then the equilibrium* $(0, 0, C/\beta)$ *is locally stable when* $C > C_*$*, and it is unstable when* $0 < C < C_*$*. Moreover when* $0 < C < C_*$*, the system has at least one positive equilibrium point.*

The critical value $C = C_*$ is a bifurcation point where a branch of nontrivial equilibrium points emanates from the line of trivial equilibria $(C, O, B, S) = (C, 0, 0, C/\beta)$. The bifurcation is called subcritical if the branch of bifurcating positive equilibria bends to the left of $C = C_*$, otherwise it is supercritical.

3.3 Supercritical versus Subcritical Bifurcations

In this section we explain the method of bifurcation of equilibrium points from a know branch of trivial equilibria. It is well-known as "bifurcation from a simple eigenvalue" in the studies of analytical bifurcation theory (see [2, 3, 11, 18]). Here we apply this powerful method to a finite-dimensional problem.

Consider a smooth mapping $F = F(\lambda, u) : \mathbf{R} \times U \to \mathbf{R}^n$ where U is an open subset of $\mathbf{R}^n$, $n \geq 1$, λ is a parameter and u is the state variable. We consider the equilibrium problem

$$F(\lambda, u) = 0. \tag{3.14}$$

Assume that a trivial solution is known. That is, there exists $u_0 \in U$ so that $F(\lambda, u_0) = 0$ for all $\lambda \in \mathbf{R}$. So $\{(\lambda, u_0) : \lambda \in \mathbf{R}\}$ is a line of trivial solutions of (3.14).

The linearization of F with respect to u is represented by the Jacobian matrix: $F_u = (J_{ij} = \partial_j F_i)$, where J_{ij} is the entry of F_u at row i and column j, and

$$\partial_j F_i = \frac{\partial F_i(\lambda, u)}{\partial u_j}, \quad 1 \leq i, j \leq n,$$

is the partial derivative. Note that $F = (F_1, F_2, \cdots, F_n)$ and $u = (u_1, u_2, \cdots, u_n)$ are both vectors in $\mathbf{R}^n$. Similarly the second derivative of F on u is expressed as a 3-dimensional matroid $F_{uu} = (K_{ijk} = \partial_{jk} F_i)$, where

$$\partial_{jk} F_i = \frac{\partial^2 F_i(\lambda, u)}{\partial u_j \partial u_k}, \quad 1 \leq i, j, k \leq n,$$

is the second order partial derivative. Also the mixed derivative $F_{\lambda u} = (M_{ij} = \partial_{\lambda j} F_i)$

where

$$\partial_{\lambda j} F_i = \frac{\partial^2 F_i(\lambda, u)}{\partial u_j \partial \lambda}, \quad 1 \le i, j \le n.$$

We notice that F_u defines a linear operator $\mathbf{R}^n \to \mathbf{R}^n$ with matrix multiplication, so is $F_{\lambda u}$; and F_{uu} defines a bilinear operator $\mathbf{R}^n \times \mathbf{R}^n \to \mathbf{R}^n$ which can be expressed as

$$F_{uu}[(x_1, \cdots, x_n), (y_1, \cdots, y_n)] = (\sum_{j,k} K_{1jk} x_j y_k, \cdots, \sum_{j,k} K_{njk} x_j y_k).$$

Finally for a linear operator $L : \mathbf{R}^n \to \mathbf{R}^n$, we use $N(L)$ and $R(L)$ to denote the null space and the range of L; and we use $\langle x, y \rangle$ to denote the standard dot product of $x, y \in \mathbf{R}^n$.

Now we are ready to state a bifurcation theorem due to Crandall and Rabinowitz [3] (here we only state a special case):

Theorem 3.2. *Let $F : \mathbf{R} \times U \to \mathbf{R}^n$ be twice continuously differentiable, where U is an open subset of $\mathbf{R}^n$. Suppose that $F(\lambda, u_0) = 0$ for $\lambda \in \mathbf{R}$, and at (λ_0, u_0), F satisfies*

(F1) *$dim N(F_u(\lambda_0, u_0)) = codim R(F_u(\lambda_0, u_0)) = 1$, and $N(F_u(\lambda_0, u_0)) = Span\{w_0\}$;*

(F3) *$F_{\lambda u}(\lambda_0, u_0)[w_0] \notin R(F_u(\lambda_0, u_0))$.*

Then the solutions of (3.14) near (λ_0, u_0) consists precisely of the curves $u = u_0$ and $(\lambda(s), u(s))$, $s \in I = (-\delta, \delta)$, where $(\lambda(s), u(s))$ are continuously differentiable functions such that $\lambda(0) = \lambda_0$, $u(0) = u_0$, $u'(0) = w_0$. Moreover

$$\lambda'(0) = -\frac{\langle l, F_{uu}(\lambda_0, u_0)[w_0, w_0] \rangle}{2\langle l, F_{\lambda u}(\lambda_0, u_0)[w_0] \rangle}, \tag{3.15}$$

where $l \in \mathbf{R}^n$ satisfying $R(F_u(\lambda_0, u_0)) = \{y \in \mathbf{R}^n : \langle l, y \rangle = 0\}$.

In laymans terms, at a bifurcation point $\lambda = \lambda_0$, the Jabobian F_u has zero as an eigenvalue; **(F1)** means that zero is a simple eigenvalue of F_u, which means that the eigen-space of F_u is one-dimensional, and the range of F_u is $(n-1)$-dimensional (called, codimension one); **(F3)** means that $F_{\lambda u}[w_0]$ does not belong to the range of F_u, where w_0 is any nonzero eigenvector. Once these conditions are satisfied, then there is a curve of

solutions bifurcating from the branch of trivial solutions. The formula of $\lambda'(0)$ is useful for determining the direction of the bifurcation (sub/supercritical).

To apply the above abstract theory to our problem, we notice that the trivial equilibria $(C, O, B, S) = (C, 0, 0, C/\beta)$ is not constant for C. Hence we make a change of variable $z = S - C/\beta$ then $(O, B, z) = (0, 0, 0)$ is a constant solution. We define

$$G(C, O, B, z) = \begin{pmatrix} rOf(d)\left(1 - \dfrac{O}{k}\right) - \mu f(d)O - \epsilon(1 - f(d))O \\ rf(d)\dfrac{O^2}{k} + \mu f(d)O - \gamma B + \epsilon(1 - f(d))O \\ Cge^{-\frac{FO}{Cg}} - \beta z - C \end{pmatrix}, \tag{3.16}$$

where $d = \lambda(O/2 + B) - z - C/\beta$, and definitions of f, k, g, F are same as before. Let $u = (O, B, z)$. Then $G_u(C, 0, 0, 0)$ is the same as (3.12). At $C = C_*$, $G_u(C_*, 0, 0, 0)$ can be written as

$$L \equiv G_u(C_*, 0, 0, 0) = \begin{pmatrix} 0 & 0 & 0 \\ \dfrac{\epsilon r}{r - \mu + \epsilon} & -\gamma & 0 \\ C_* g'(0) - F(C_*) & C_* g'(0) & -\beta \end{pmatrix}. \tag{3.17}$$

We take the eigenvector of L to be $w_0 = (1, w_{02}, w_{03})$ where

$$\begin{aligned} w_{02} &= \frac{\epsilon r}{\gamma(r - \mu + \epsilon)}, \\ w_{03} &= \frac{C_* g'(0) - F(C_*)}{\beta} + \frac{C_* g'(0)\epsilon r}{\beta\gamma(r - \mu + \epsilon)}, \end{aligned}$$

one can see that the range of L is $\{(0, y, z) \in \mathbf{R}^3\}$ which is two-dimensional, so we can take the vector l to be $(1, 0, 0)$. A vector v does not belong to the range of L if the first entry of v is not zero. So to apply (3.15), we *only* need to calculate the derivatives from the first equation of the system.

We can calculate that $\langle l, G_{\lambda u}(C_*, 0, 0, 0)[w_0] \rangle = -f'(-C_*/\beta)(r - \mu + \epsilon)/\beta < 0$, and

with a more tedious calculation, we find that

$$\begin{aligned}&\langle l, F_{uu}(\lambda_0, u_0)[w_0, w_0]\rangle \\ =&\frac{2r}{k} f'(-C_*/\beta)\left[\frac{\lambda(r-\mu+\epsilon)k}{2r} - \frac{f(-C_*/\beta)}{f'(-C_*/\beta)} + \frac{\lambda\epsilon k}{\gamma} - \frac{\epsilon k}{\gamma\beta}\left(C_* g'(0) - F(C_*) + \frac{C_* g'(0)\epsilon r}{\gamma(r-\mu+\epsilon)}\right)\right].\end{aligned} \tag{3.18}$$

Hence combining all the calculations, we find that the direction of the branch of bifurcating positive equilibria is determined by

$$I = \frac{\lambda(r-\mu+\epsilon)k}{2r} - \frac{f(-C_*/\beta)}{f'(-C_*/\beta)} + \frac{\lambda\epsilon k}{\gamma} - \frac{\epsilon k}{\gamma\beta}\left(C_* g'(0) - F(C_*) + \frac{C_* g'(0)\epsilon r}{\gamma(r-\mu+\epsilon)}\right). \tag{3.19}$$

So the direction of the branch of bifurcating positive equilibria is determined by the quantity I defined above. If $I < 0$, then the bifurcation is subcritical and a unique equilibrium exists for $0 < C < C_*$, and there is no equilibrium for $C > C_*$; on the other hand, if $I > 0$, then the bifurcation is supercritical, then there is a range of values of $C > C_*$ for which the system has two equilibria. It is easy to observe that when the maximum sediment deposition rate C is large, then the system (2.12)-(2.14) can only have the trivial equilibrium.

Therefore the question of bistability for certain parameter range is reduced to whether $I > 0$. Notice that $g'(0) < 0$ and $F(C_*) > 0$, hence

$$I_1 = \frac{\lambda(r-\mu+\epsilon)k}{2r} + \frac{\lambda\epsilon k}{\gamma} - \frac{\epsilon k}{\gamma\beta}\left(C_* g'(0) - F(C_*) + \frac{C_* g'(0)\epsilon r}{\gamma(r-\mu+\epsilon)}\right) > 0,$$

and the positivity of $I = I_1 - I_2$ depends on the competition between I_1 and $I_2 = \dfrac{f(-C_*/\beta)}{f'(-C_*/\beta)} > 0$. Here I_2 only depends on the form of f and C_*/β, while I_1 depends on many other parameters. Notice that C_* is determined by f and $\dfrac{r-\mu+\epsilon}{\epsilon}$. If we fix the values of r, μ, ϵ, and β, then one can increase I_1 by (i) increasing carry capacity k; (ii) increasing the packing density λ; (iii) decreasing the oyster shell degrading rate γ; (iv) increasing $|g'(0)|$, decay rate of sediment deposition on the reef height; or (v) increasing $F(C_*)$, which indicates the oyster filtration ability. Hence we have identified five ways to achieve bistability in the system.

3.4 Numerical Calculations

To illustrate our results, numerically calculate our model and also compare with field data, we now explicitly define the functions $f(d)$, $g(x)$, and $F(y)$. We use the following set of desired functions satisfying the conditions (2.2), (2.6), (2.7):

$$\begin{aligned} f(d_0) &= \frac{1}{1+e^{-hd_0}}, \quad d_0 = d - \frac{\lambda O}{2} \\ g(x) &= e^{-\eta x}, \quad (g(O+B) = e^{-\eta(O+B)}), \\ F(y) &= Mye^{-\theta y}, \quad (F(Cg) = MCge^{-\theta Cg}). \end{aligned} \tag{3.20}$$

Here $h > 0$ is a parameter which adjusts the shape of the sigmoid function f—for larger h, the sigmoid function f has narrower transition layer where the function value jumps from 0 to 1. $\frac{\lambda O}{2}$ is subtracted from d in order to shift the sigmoid function so that $f(0) \approx 0$ and $f(O) \approx 1$). In the definition of g, η is the decay rate of the exponential function; the per volume filtration rate $F = F(Cg)$ is a function on Cg, and the form of the function $F(y)$ is of Ricker type, where M represents the maximum filtration rate, and θ is a decay rate. Notice that $F(y)$ achieves its maximum value at $y = 1/\theta$, and the maximum value is $M/(e\theta)$. Hence to achieve an effective maximum filtration rate of F_0, one needs to select $M = e\theta F_0$.

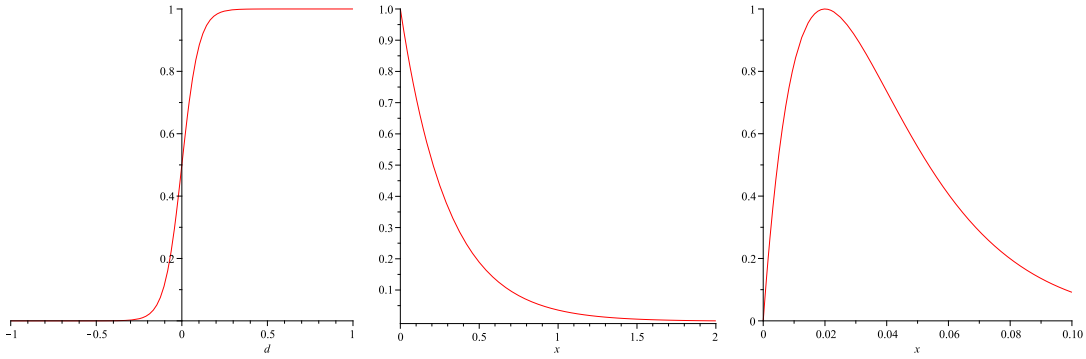

Figure 3.1: Graphs of functions $f(d)$, $g(x)$ and $F(y)$ defined in (3.20). (left) $f(d)$ with $h = 1$; (middle) $g(x)$ with $\eta = 10/3$; (right) $F(y)$ with $\theta = 50$ and $M = \theta e$.

With the nonlinear functions f, g and F defined as in (3.20), we assume the following set of parameters:

Parameter	λ	r	k	μ	ϵ	γ	η	θ	M	β	h	C
Value	1	1	0.3	0.4	0.94	0.7	3.33	50	$50e$	0.01	20	0.02

Table 3.1: A sample set of reasonable parameters

Then we obtain two equilibrium points $(O_1, B_1, S_1) = (0.0566, 0.0456, 0.0326)$ and $(O_2, B_2, S_2) = (0.1736, 0.1022, 1.0645 \times 10^{-7})$, and see Fig. 3.2 left panel for an illustration of the two intersecting curves $L(O)$ and $R(O)$ defined in (3.10). Freeing the parameter C gives a bifurcation diagram (see Fig. 3.2 right panel) with a "bend back" curve. The curve continues to $C = 0$ with a positive O-value, that corresponds to an equilibrium point when $C = 0$: $(O^*, B^*, 0)$ where O^* satisfies

$$f\left(\lambda\left(\frac{O}{2} + B(O)\right)\right) = \frac{\epsilon k}{k(r - \mu + \epsilon) - rO}. \tag{3.21}$$

Here the bifurcation point $C_* = 2.24 \times 10^{-4}$ is very small. On the other hand, there is a saddle-node bifurcation point $C^* \approx 0.078$ where the curve bends back. For all C values in (C_*, C^*), there are two positive equilibria.

We use some numerical simulation to have a close look at the bistable dynamics of (3.1)-(3.3) with parameters given in Table 3.1. We use the initial value of $O(0) = 0.01$ and $S(0) = 0.01$, that is, there is a small amount of live oyster and also a small amount of sediment initially. We choose several different values of $B(0)$: $B(0) = 0.20$, 0.10, 0.12 and 0.11 (see Fig. 3.3). Then it is clear that for larger $B(0)$, the oyster population survives and reach the large stable equilibrium (O_1, B_1, S_1), while the smaller $B(0)$ will drive the oyster population to zero equilibrium. The critical level of original reef height $B(0)$ is between 0.11 and 0.12. Observing the transient dynamics with $B(0) = 0.12$ and $B(0) = 0.11$ when $0 \le t \le 10$ (see Fig. 3.4), one can see that with slightly higher reef, the

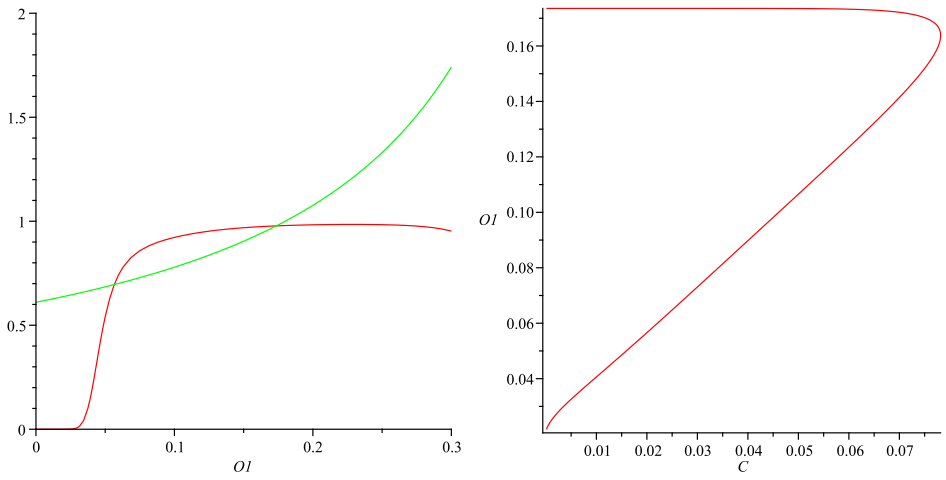

Figure 3.2: Equilibrium solutions and bifurcation, with parameters given in Table 3.1. (left) The graph showing the intersection of the two curves $L(O)$ and $R(O)$. Here the horizontal axis is O, and the vertical axis is the function values; (right) bifurcation diagram of (3.1)-(3.3). Here the horizontal axis is C, and the vertical axis is O.

live oyster volume is able to keep increasing, and eventually curbs the sediment volume to a very small value with the filtration function; on the other hand, with slightly lower reef, the live oyster cannot keep up with the rising sediment, and the sediment later covers both the live and dead oyster.

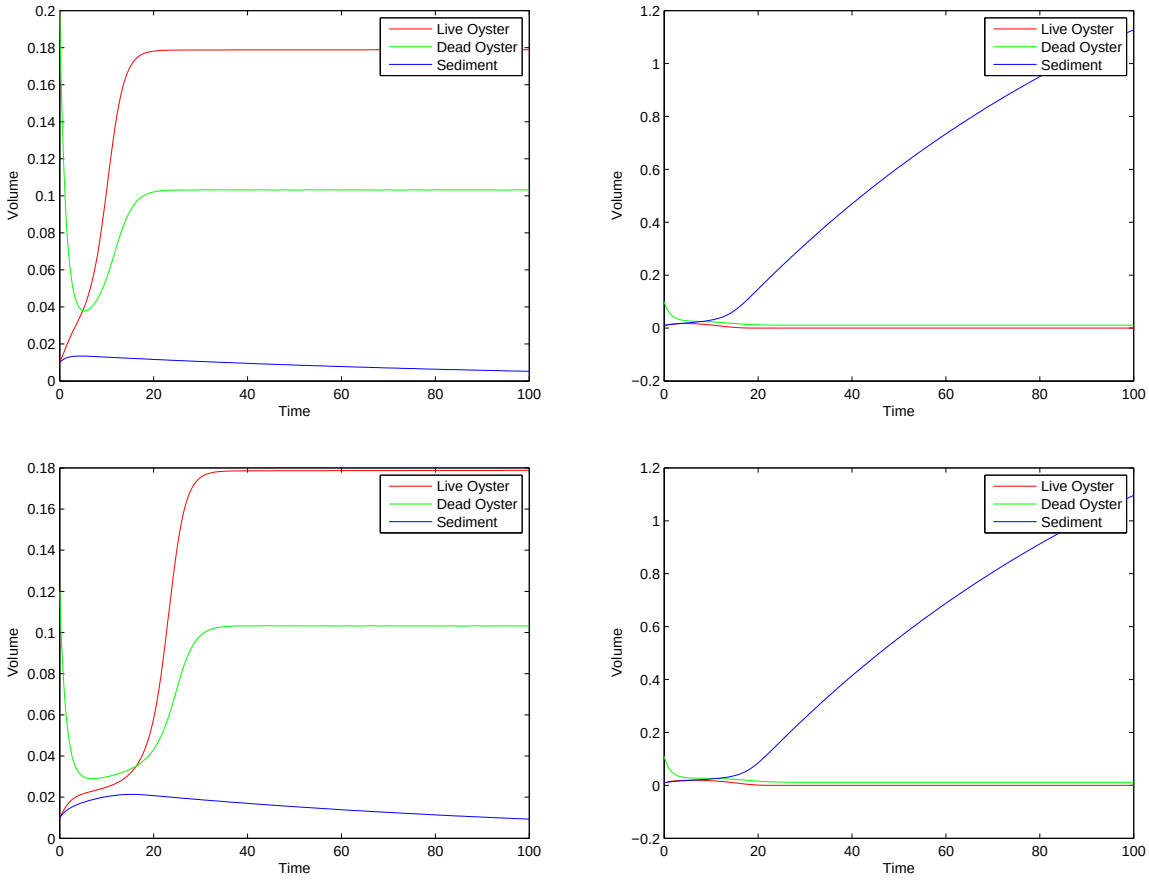

Figure 3.3: Numerical solution ($0 \leq t \leq 100$) of (3.1)-(3.3) with parameters given in Table 3.1. For all cases $O(0) = 0.01$ and $S(0) = 0.01$. (upper left) $B(0) = 0.20$; (upper right) $B(0) = 0.10$; (lower left) $B(0) = 0.12$; (lower right) $B(0) = 0.11$.

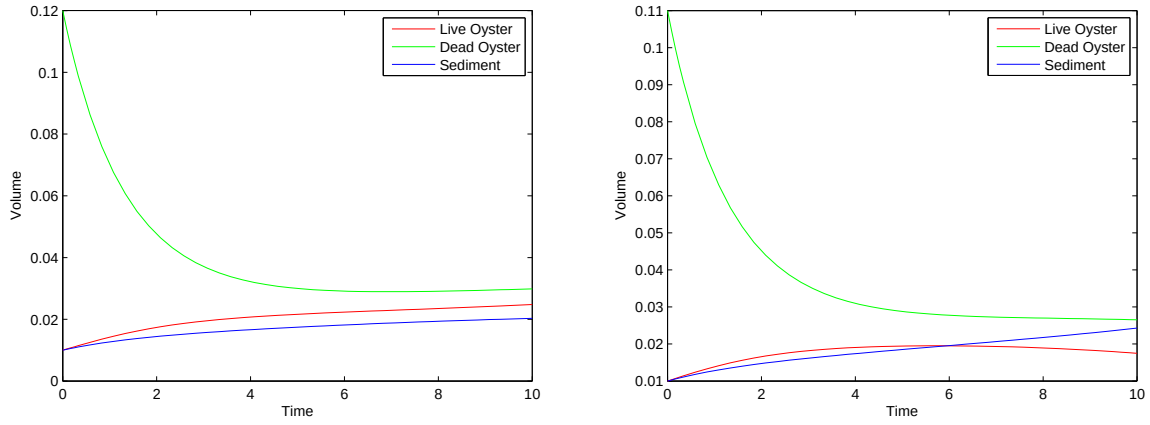

Figure 3.4: Numerical solution ($0 \leq t \leq 10$) of (3.1)-(3.3) with parameters given in Table 3.1. (left) Initial value $O(0) = 0.01$, $B(0) = 0.12$ and $S(0) = 0.01$; (right) Initial value $O(0) = 0.01$, $B(0) = 0.11$ and $S(0) = 0.01$

3.5 Matlab code for Numerical Simulation

```
function WillBistability2


%parameters
%intervals of time which to run the model
tspan=[0 400];
%the initial condition for y0 = [O, B, S]
y0=[0.02; 0.15; 0.01];
r=1;          %birth minus death by competition rate
K=.3;         %oyster capacity
mu=0.4;       %natural death rate
ep=0.94;      %death rate of submerged oyster
lambda=1;     %packing density
H=10;         %scaling factor
```

```
gamma=0.15;  %oyster shell degradation rate
M=0.24;      %maximum sediment filtration
C=0.02;      %maximum sediment deposition rate
theta=1;     %sediment amount where filtration is maximum
eta=1/0.3;   %decay rate of sediment deposition on the reef height
beta=0.01;   %sediment erosion rate

[T,Y]=ode45(@f,tspan,y0);
set(gcf,'DefaultAxesColorOrder',[1 0 0;0
10;0 0 1]) plot(T,Y);
xlabel('Time');
ylabel('Volume');
legend('Live Oyster', 'Dead Oyster', 'Sediment')

function dy=f(t,y)

fd=1/(1+exp(-H*(lambda*(y(1)+y(2))-y(3))));
gx=exp(-eta*lambda*(y(1)+y(2)));
Fx=M*C*gx*exp(-theta*C*gx);

dy = zeros(3,1);    % a column vector
dy(1) = r*y(1)*fd*(1-y(1)/K)-mu*y(1)*fd-ep*(1-fd)*y(1);
dy(2)=mu*y(1)*fd-gamma*y(2)*fd+ep*(1-fd)*y(1);
dy(3)=C*gx*exp(-Fx*y(1)/C/gx)-beta*y(3);

end
end
```

3.6 Maple code for Symbolic Calculations

```
restart:with(plots): with(linalg):

%Define mechanistic functions
g:=exp(-eta*lambda*(O+B));
F:=M*C*g*exp(-theta*C*g); d:=lambda*(O/2+B)-(z+C/beta);
fd:=1/(1+exp(h*d));

%Define change in state variables with general f(d) and S = z +C/beta
u1:= r*O*f(d)*(1-O/K)-mu*O*f(d)-epsilon*(1-f(d))*O;
u2:=mu*O*f(d)-gam*B+epsilon*(1-f(d))*O;
u3:=C*g*exp(-F*O/(C*g))-beta*(z+C/beta);

%Define state variables with general f(d)
ds :=lambda*(O/2+B)-S;
u1S:= r*O*f(ds)*(1-O/K)-mu*O*f(ds)-epsilon*(1-f(ds))*O;
u2S:=mu*O*f(ds)-gam*B+epsilon*(1-f(ds))*O;
u3S:=C*g*exp(-F*O/(C*g))-beta*(S);

%Compute Jacobian with general F(y), g(x), and f(d) at trivial solution
jacobian([u1S, u2S, u3S],[O,B,S]);
subs({O = 0, B = 0, S = C/beta}, %);

%Compute lambda0
u1fd:= r*O*fd*(1-O/K)-mu*O*fd-epsilon*(1-fd)*O;
topleftentry := diff(u1fd,O);
topleftentry := subs({O = 0, B = 0, z = 0}, %);
```

```
topleftentry = simplify(%);
lambda0 := solve(topleftentry,C);

%Compute w0
u2fd:= mu*O*fd-gam*B+epsilon*(1-fd)*O;
u3fd:=C*g*exp(-F*O/(C*g))-beta*(z+C/beta);
jacobian([u1fd, u2fd,u3fd],[O,B,z]);
Futriv:=subs({O=0, B=0, z=0, C = lambda0}, %);
Futriv:=simplify(%);
w0 := nullspace(Futriv);

%Compute u1 component matrix of matroid Fuu(lambda0, u0)
hessian(u1,[O,B,z]);
Fuutriv := subs({O=0, B=0, z=0, C = lambda0}, %);
Fuutruv := simplify(%);

%Compute u1 component of vector Fuu(lambda0, u0)[w0,w0]
A :=gam*(epsilon+r-mu)/(r*epsilon);
B:=ln((r-mu)/epsilon)*(eta*lambda*r*epsilon+gam*eta*lambda*epsilon+gam*eta*lambda*r
   -gam*eta*lambda*mu+gam*M*((r-mu)/epsilon)^(theta*beta/h)*epsilon
   +gam*M*((r-mu)/epsilon)^(theta*beta/h)*r
   -gam*M*((r-mu)/epsilon)^(theta*beta/h)*mu)/(h*r*epsilon);
A*(A*Fuutriv[1,1]+Fuutriv[2,1]+B*Fuutriv[3,1]) + A*Fuutriv[2,1]+A*B*Fuutriv[3,1];
numtor := simplify(%);

%Compute <l, F_u(u0, u0) *w0>
u1c:=diff(u1,C);
```

```
u2c:=diff(u2,C);
u3c:=diff(u3,C);
jacobian([u1c, u2c, u3c],[O,B,z]);
Fcutriv:=subs({O=0, B=0, z=0, C = lambda0}, %);
Fcutriv[1,1]*A;
dentor := simplify(%);

%Compute I = -1/2 * numerator over denominator
-1/2*numtor/(-(D(f))(-lambda0/beta)*(epsilon+r-mu)*A/beta);
simplify(%)
```

Chapter 4

Conclusions

Let us first briefly review the purpose of this paper. The Chesapeake Bay oyster is the natural filter of its home. Perched upon high reefs, they historically maintained suspended sediments and nutrients at levels conducive to abundant marine life. However, human activity has hampered their ability to provide this vital service. Oysters populations have been decimated. Additionally, the vertical relief of reefs has been reduced, exposing oysters to higher suspended particle density. Sediment in the present densities is harmful to oysters, reducing fecundity and raising mortality. Faced with harvest pressure and growing sediment densities, oyster populations have continued to decline.

Efforts to curb this decline and restore oysters to higher population levels have been largely ineffectual. Reefs are built and populated with oysters but after a few years, most disappear. However, high relief reefs from the Great Wicomico River experiment have survived and flourished. Low relief reefs in the same area have been considerably less successful and have largely returned to the state of unrestored bottom. This experimental data argues for the existence of alternative stables states in which there exist critical thresholds that separate different zones of attraction. Analogous to the system within shallow lakes, the Bay can exist in a state of low turbity (suspended sediment) and high oyster volume. However, if a critical threshold of external and internal conditions are

passed, the Bay will go to a state of high turbity and low oyster volume.

We set out to provide theoretical evidence that the negative effect of sediment of oysters and oyster filtration of sediment formed a feedback mechanism that could produce alternative stables states. We constructed a model of three ordinary differential equations to track the change in live oyster, dead oyster, and sediment volume. Live oyster volume grew according to logistic growth with a natural death rate and a death term due to submersion in sediment. We tracked dead oyster volume which live oyster grow on to elevate themselves above sediment which concentrates on the Bay floor. Sediment volume grew according to a delinearization of a standard model for sediment accumulation minus the amount filtered by oysters. Using several techniques, we concluded that the model contained multiple nonnegative equilibria.

Setting the change in our system to zero, we solved for the value of live oysters at equilibria. In addition to the trivial solution, we discovered a range of parameters on which multiple equilibria exist. Specifically, we discovered there exist two bifurcation values of the parameter representing maximum sediment deposition, C. The bifurcation diagram of C and O closely resembles the common S-shaped diagram featured in all papers of bistability (Figure 3.2). The figure clearly shows that multiple equilibria exist between the two bifurcation values of C.

We determined the slope of the curve as a function of the parameter values. Multiple equilibria exist for a positive slope at bifurcation curves emergence from the trivial solution. Conversely, only the trivial solution exists for a negative slope. Therefore, the existence of equilibria is dependent on the parameters and can be shown by ecologists to exist for an ecologically reasonable parameter set.

Numerical simulation done in `Matlab` using the common program `ode45` contributes more evidence. Parameters can be easily manipulated within and outside the ecologically reasonable range. For a wide range of parameter values for which ecologically reasonable range is a subset, the long term behavior of solution curves is dependent on the initial

value of the dead oysters. Therefore, for each reasonable choice of parameter values, there exists a value of $B(0)$ such that above this value, live oyster volume will approach a positive equilibrium and sediment volume will approach a negligible amount. Conversely, below this value of $B(0)$, sediment will overwhelm live oysters and they will approach the trivial solution. This result explains the success of high relief reefs and the failure of low relief reefs in the Great Wicomico River.

In summary, there is now experimental and theoretical evidence for the existence of alternative stable states in the system of oyster reefs and sediment in the Bay. The model used in this paper is basic and neglects many important factors in this real and complex system. However, it does concretely show that alternative stable states do exist from the relationship of sediment and oysters. Refinement of the model and extension of its complexity could result in accurate prediction of the real system and provide insight into the required heights of artificial reefs for successful restoration.

4.1 Afterward

"The world is your oyster."

These are beautiful and inspiring words. As I face impending graduation, uncertainty and fear of the broad unknown threatens my aspirations. For one who has been training in the quest of certainty and objective truth, the broad expanse of paths before my feet could immobilize me. But the world is indeed my oyster. Fear turns to excitement and the unknown reveals itself as endless possibility.

My work on this thesis has also given me another perspective with which to view these words. These oysters, that we have joyfully devor in our country's youthful spirit, are almost gone now. They have yielded themselves to our pleasure and given all they had. Now like a confused child after a plaything has been broken, we sit back and wonder. We have the power to destroy these oysters, the bounty of the earth laid prone in our palms. We have the power to destroy this entire world. Thankfully, we also the power to protect

it and if we are granted any meaning in this life, it is exercise that power.

4.2 Acknowledgements

Thank you to Douglas Price for instructing me in my first college math course, Calculus I, in the spring of my sophomore year.

Thank you to Paul Tian for encouraging me to take Math 345, Biological Mathematics, and getting me involved with Romuald Lipcius. Thank you Romuald Lipcius for giving me a project to work on. Thank you again to Paul Tian for encouraging me to apply for CSUMS and UBM funding.

Thank you to NSF for providing me support under the UBM and CSUMS grants. Upwards of $10,000$ thanks to Romuald Lipcius and the Virginia Institute of Marine Science for paying the tuition of my Fall 2009 and Spring 2010 semesters.

Endless mountains of gratitude to my advisors, Leah Shaw, Jian Shen, Romuald Lipcius, and Junping Shi. I appreciate the opportunity afforded a babe in this industry.

Special thanks to Junping Shi who is the most laid back and helpful professor at William and Mary.

For support, I must thank my parents and family and Yael Gilboa.

Bibliography

[1] Chapra, S.C., 1997. Surface Water-Quality Modeling. McGraw-Hill, New York, USA, pp. 844.

[2] Chow, Shui Nee; Hale, Jack K., 1982. Methods of bifurcation theory. Springer-Verlag, New York-Berlin.

[3] Crandall, Michael G.; Rabinowitz, Paul H., 1971. Bifurcation from simple eigenvalues. *Jour. Func. Anal.*, **8**, 321–340.

[4] Dong, Quan; McCormickb, Paul V.; Sklarb, Fred H.; DeAngelis, Donald L., 2002. Structural Instability, Multiple Stable States, and Hysteresis in Periphyton Driven by Phosphorus Enrichment in the Everglades. *Theo. Popu. Biol.* **61**, No. 1, 1–13.

[5] Fountain, Henry, "Oysters Are on the Rebound in the Chesapeake Bay", New York Times, August 4, 2009.

[6] Guill, Christian, 2009. Alternative dynamical stages in stage-structured consumer populations, *Theoretical Population Biology.* **76**: 168-178.

[7] Hadeler, K.P.; Van den Driessche, P., 1997. Backward bifurcation in epidemic control. *Mathem. Biosci.* **146**, No. 1, 15–35.

[8] Ji, Z., 2007. Hydrodynamics and water quality: modeling Rivers, lakes and estuaries. Wiley-Interscience, United States of American, pp. 676.

[9] Jiang, Jifa; Shi, Junping, 2009. Bistability dynamics in some structured ecological models. In *Spatial Ecology* (Chapman & Hall/CRC Mathematical and Computational Biology), edited by Robert Stephen Cantrell, Chris Cosner, and Shigui Ruan, Chapman & Hall/CRC, 33–62.

[10] Lenihan, H.S., F. Micheli, S.W. Shelton, and C.H. Peterson, 1999. The influence of multiple environmental stressors on susceptibility to parasites: an experimental determination with oysters. *Limnology and Oceanography.* **44** 910–924.

[11] Liu, Ping; Shi, Junping; Wang, Yuwen, 2007. Imperfect transcritical and pitchfork bifurcations. *Jour. Func. Anal.*, **251**, No. 2, 573–600.

[12] Newell R. I. E., 1988. Ecological changes in Chesapeake Bay: are they the result of overharvesting the eastern oyster (Crassostrea virginica)? *In: Lynch MP, Krome EC (eds) Understanding the estuary. Advances in Chesapeake Bay research, Chesapeake Research Consortium.* **129**, Gloucester Point, VA, 536-546.

[13] Scheffer, M., 2009. Critical Transitions in Nature and Society. Princeton University Press, Princeton-Oxford.

[14] Scheffer, Marten; Bascompte, Jordi; Brock, William; Brovkin, Victor; Carpenter, Stephen; Dakos, Vasilis; Held, Hermann; van Nes, Egbert; Rietkerk, Max; Sugihara, George, 2009. Early-warning signals for critical transitions, *Nature.* **461**: 53-59.

[15] Scheffer, M.; Carpenter, S.R., 2003. Catastrophic regime shifts in ecosystems: linking theory to observation. *Trends Ecol. Evol.* **18**: 648–656.

[16] Scheffer, Marten; Carpenter, Steve; Foley, Jonathan A.; Folke, Carl; Walkerk, Brian, 2001. Catastrophic shifts in ecosystems. *Nature* **413** 591–596.

[17] Schulte, David M.; Burke, Russell P.; Lipcius, Romuald N., 2009. Unprecedented Restoration of a Native Oyster Metapopulation. *Science* **325** 1124–1128.

[18] Shi, Junping, 1999. Persistence and bifurcation of degenerate solutions, *Jour. Func. Anal.* **169**, No. 2, 494–531.

[19] Wiggins, Stephen, 1991. Introduction to Applied Nonlinear Dynamical Systems and Chaos. Springer, New York.